Electronic Supplementary Material (ESI) for Journal of Materials Chemistry A.

Supporting Information

Robust yet Flexible Slippery Layered Composite Surfaces with Programmable Pressure-resistance Response at Extreme Environmental Conditions

*Pengda Che, Xiao Han, Pu Guo, Xuan Wang, Shuman Cheng, Keyu Han, Lei Jiang, and Liping Heng**

Dr. P. D. Che, Dr. X. Han, Prof. L. P. Heng*, Dr. P. Guo, Dr. X. Wang, Dr. S. M. Cheng, Dr. K. Y. Han, Prof. L. Jiang
Key Laboratory of Bio-Inspired Smart Interfacial Science and Technology of Ministry of Education, Beijing Key Laboratory of Bio-Inspired Energy Materials and Devices, School of Chemistry, Beihang University, Beijing 100191, China.
Email: henglp@buaa.edu.cn

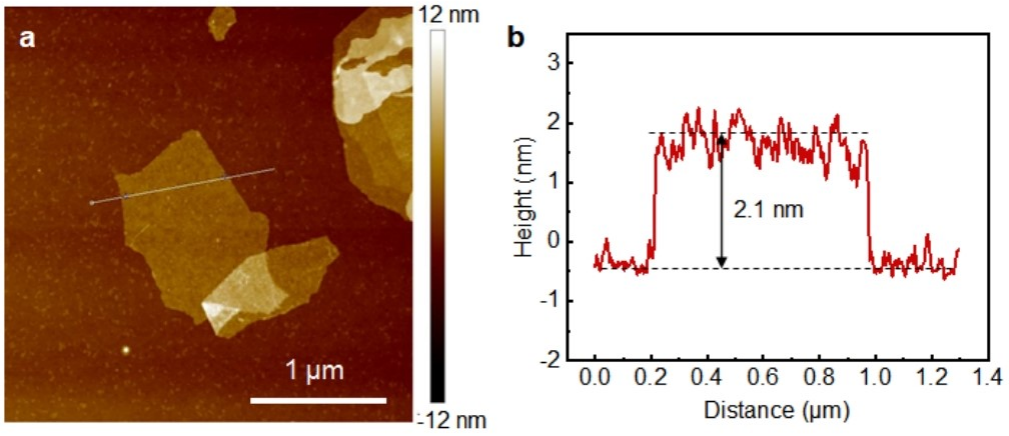

Fig. S1 (a) AFM image of the MoS_2 nanosheets on the Si substrate and (b) the corresponding height profile. The thickness of the MoS_2 nanosheets is about 2.1 nm.

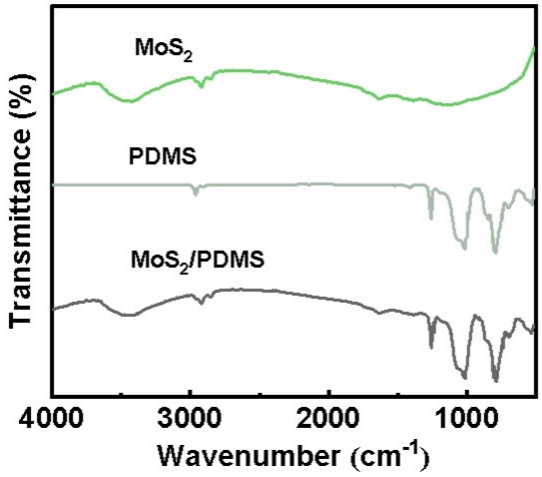

Fig. S2 FTIR spectra of MoS_2, PDMS, and MoS_2/PDMS composite.

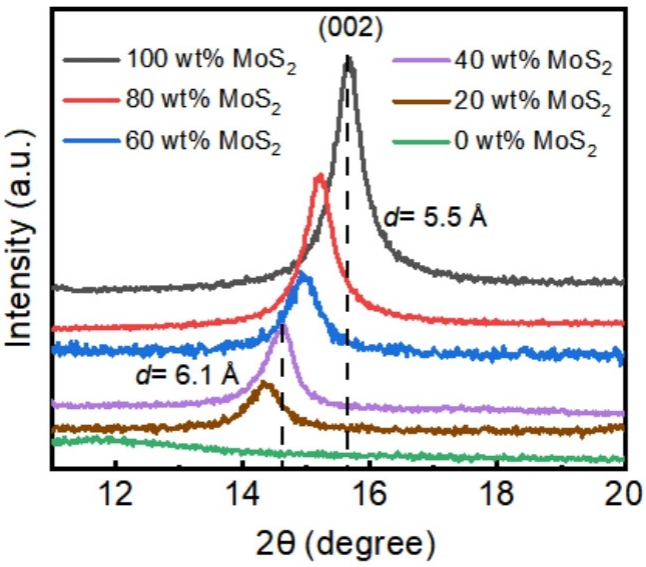

Fig. S3 XRD patterns of different samples showing the layered structures of LMP films with different layer spacing (*d*). As the MoS_2 content increases from 40 wt% to 100 wt%, *d* decreases from 6.1 Å to 5.5 Å.

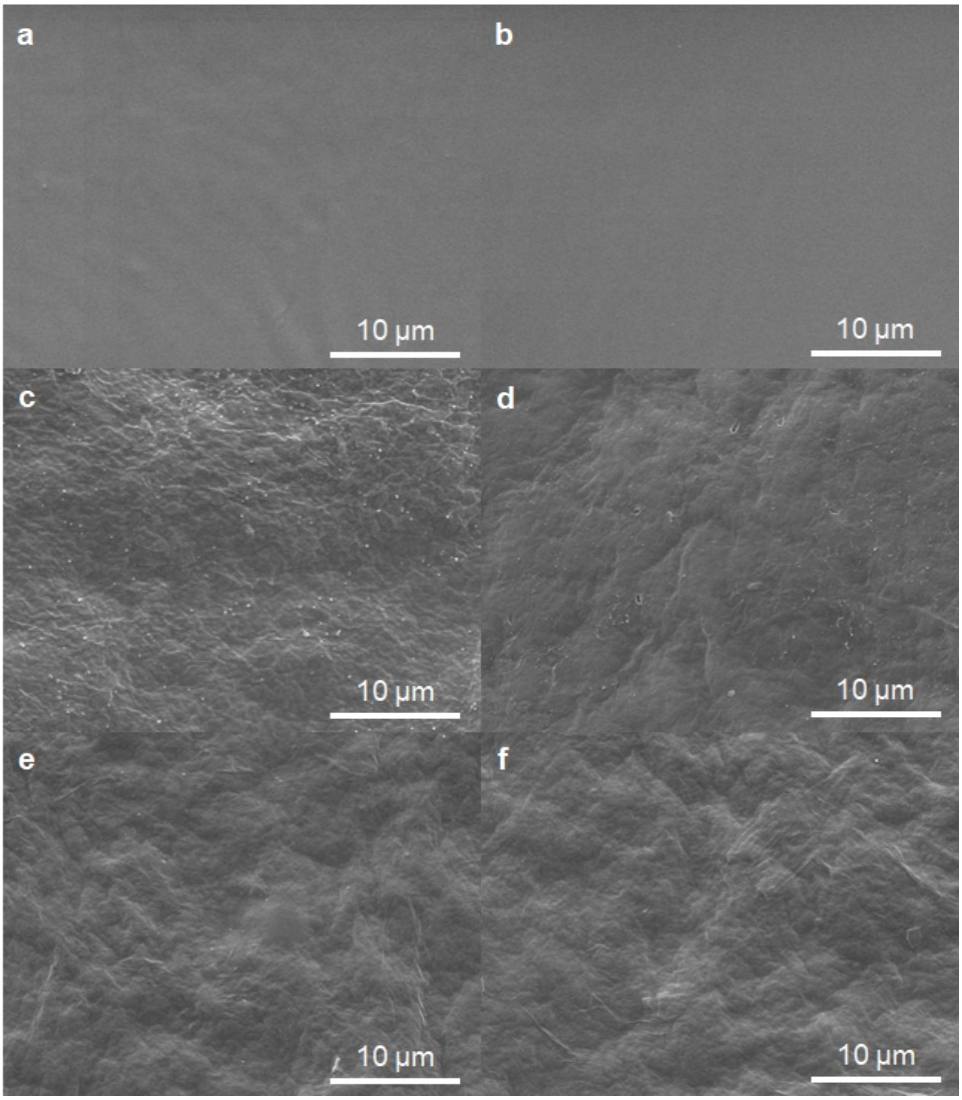

Fig. S4 Top views of LMP films prepared with different MoS_2 contents of (a) 0 wt%, (b) 20 wt%, (c) 40 wt%, (d) 60 wt%, (e) 80 wt%, and (f) 100 wt%.

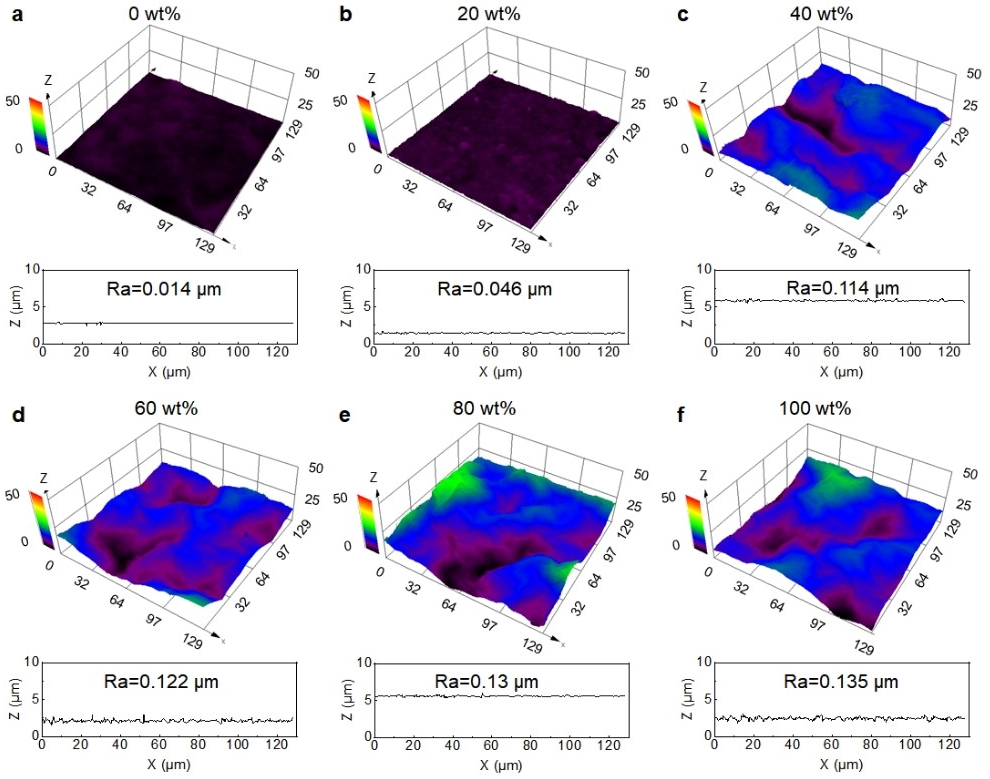

Fig. S5 3D confocal microscopy images and line profiles of the LMP films prepared with different MoS_2 contents of (a) 0 wt%, (b) 20 wt%, (c) 40 wt%, (d) 60 wt%, (e) 80 wt%, and (f) 100 wt%. The surface roughness increased with an increase of MoS_2 contents.

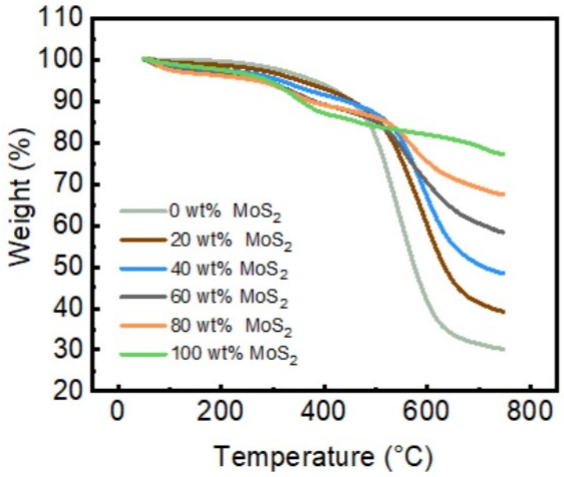

Fig. S6 Thermogravimetric analysis (TGA) of LMP films prepared with different MoS_2 content and PDMS content. The solid residue yields are about 30.2%, 39.3%, 48.5%, 58.3%, 67.4%, and 77.2% for 0 wt%, 20 wt%, 40 wt%, 60 wt%, 80 wt%, and 100 wt% MoS_2 content, respectively. Calculated by the following formula,

$$\omega \times 77.2\% + (1 - \omega) \times 30.2\% = \mathrm{m}$$

where ω is the mass fraction of MoS_2 in the LMP film, m is the theoretically calculated residual amount of solid residue. By calculation, the theoretical values of solid residue for 20 wt%, 40 wt%, 60 wt%, and 80 wt% MoS_2 content are 39.6%, 48.9%, 58.4%, and 67.8%, respectively. The theoretical and experimental values of solid residues are similar, which can prove that the content of MoS_2 and PDMS in these LMP films.

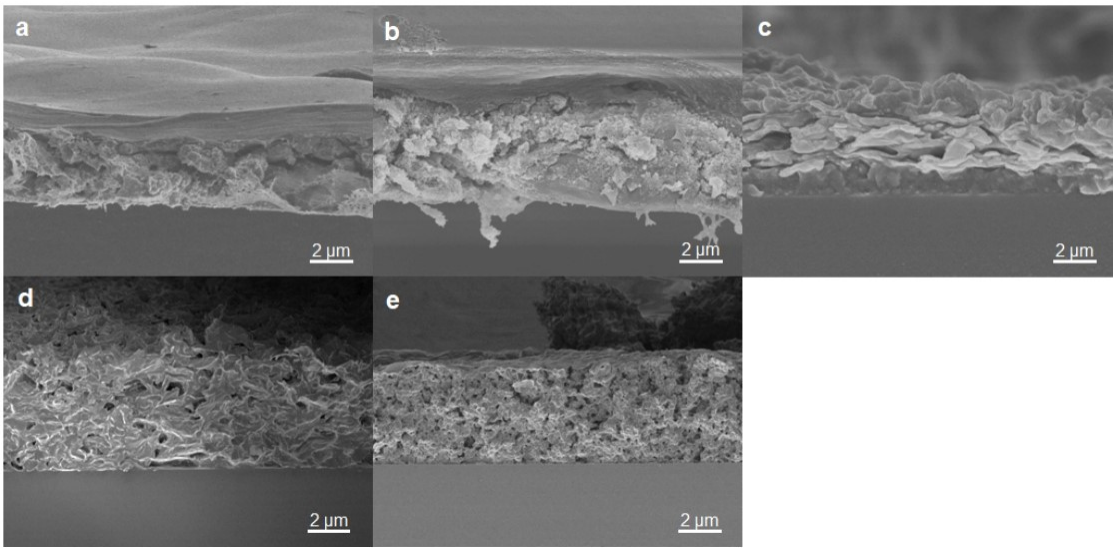

Fig. S7 Morphologies of different NLMP films. Scanning electron microscopy (SEM) images of NLMP films prepared with different MoS_2 contents of (a) 20 wt%, (b) 40 wt%, (c) 60 wt%, (d) 80 wt%, and (e) 100 wt%.

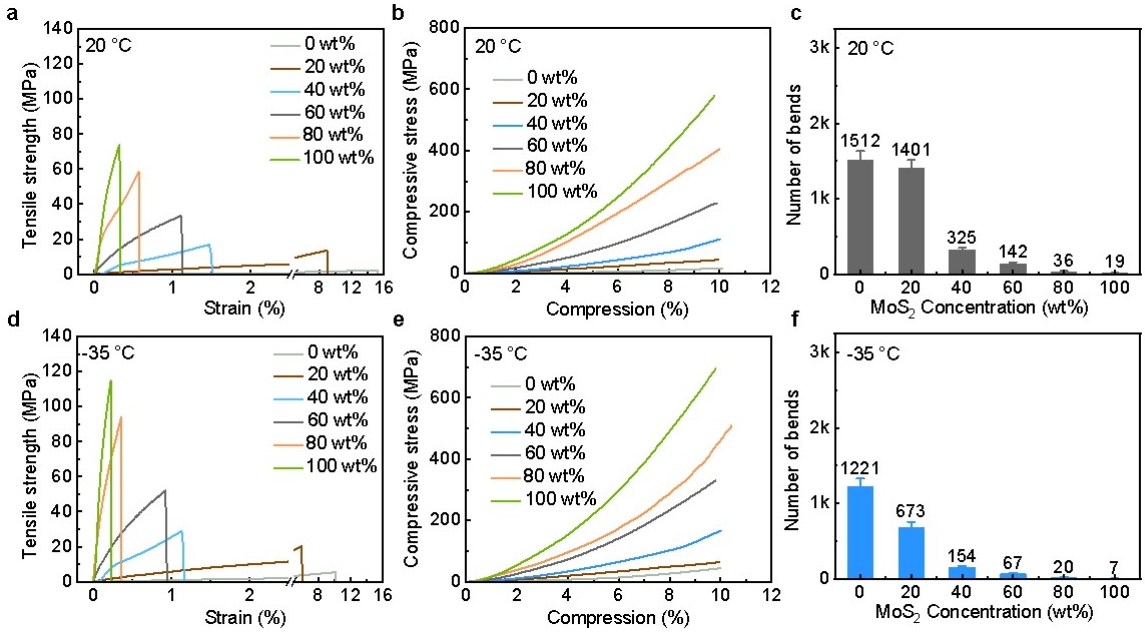

Fig. S8 Mechanical properties of different SNLMP films. (a) Tensile strength-strain curves of the SNLMP with different MoS_2 contents at 20 °C. The tensile strength properties increased with increasing MoS_2 content in the composites. (b) Compressive stress-strain curves of the SNLMP with different MoS_2 contents at 20 °C. (c) The variation of the bending times versus SNLMP films with different MoS_2 contents at 20 °C. (d) Tensile strength-strain curves of the SNLMP with different MoS_2 contents at -35 °C. (e) Compressive stress-strain curves of the SNLMP with different MoS_2 contentsat -35 °C. (f) The variation of the bending times versus SNLMP films with different MoS_2 contents at -35 °C.

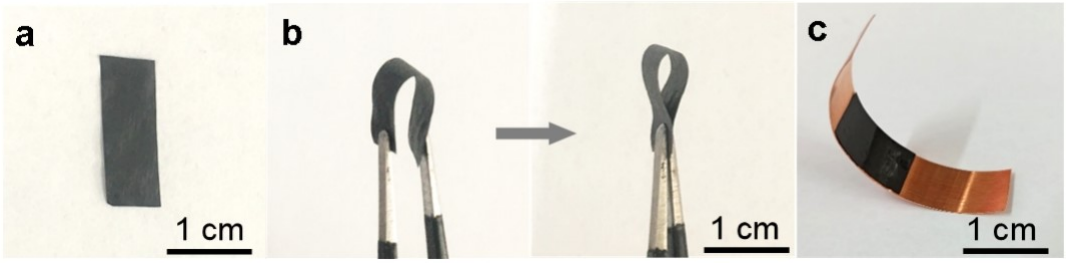

Fig. S9 (a) The optical photos of oblong SLMP films. (b) The SLMP films can be bent 180°, and can be attached to a semicircular copper electrode in (c).

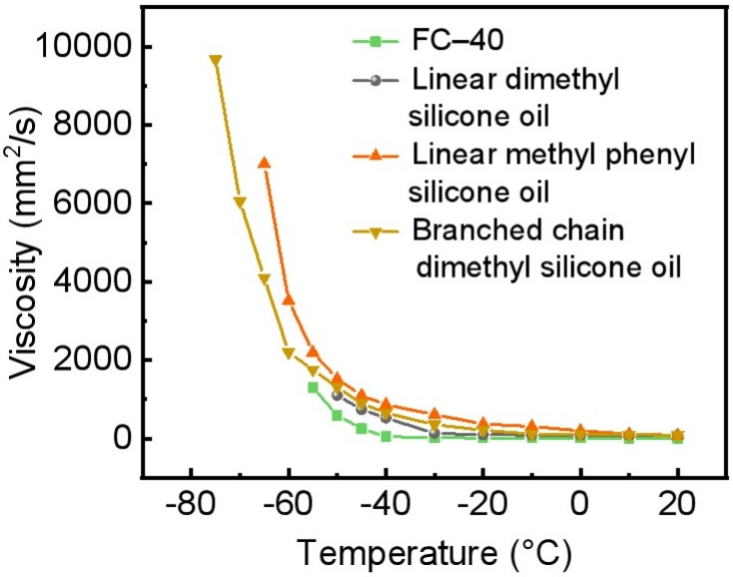

Fig. S10 Variation of viscosity with temperature for different lubricants. The viscosity increased significantly at -35, -45, -55, and -65 °C for linear dimethyl silicone oil, fluorinated liquid FC-40, linear phenyl methyl silicone oil and branched chain dimethyl silicone oil, respectively. And the freezing points of linear dimethyl silicone oil, fluorinated liquid FC-40, linear phenyl methyl silicone oil and branched chain dimethyl silicone oil are -50, -60, -70, and -80 °C, respectively.

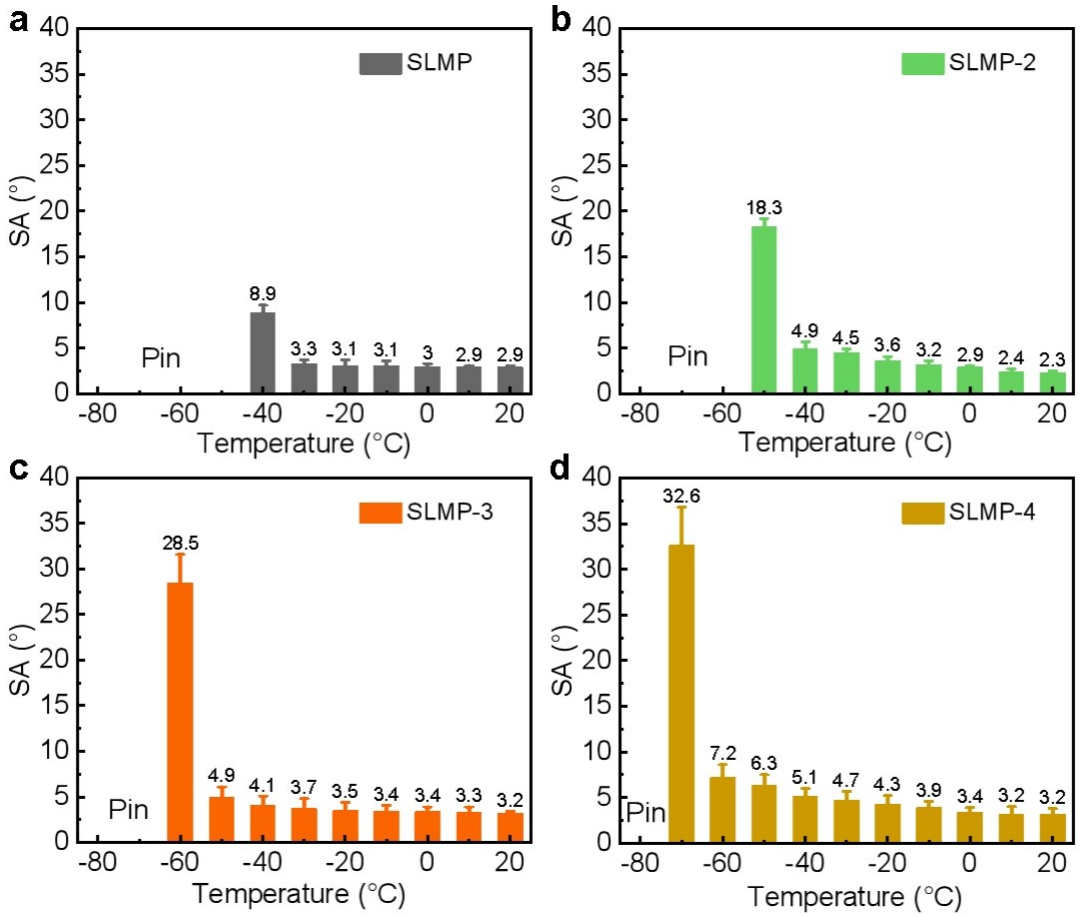

Fig. S11 Variation of SA with temperature for different SLMP films. We used LMP surfaces to adsorb different lubricants of fluorinated liquid FC-40, linear phenyl methyl silicone oil, and branched chain dimethyl silicone oil to obtain SLMP-2, SLMP-3, and SLMP-4, respectively. The SA increased notably at temperatures below -35, -45, -55, and -65 °C for (a) SLMP, (b) SLMP-2, (c) SLMP-3 and (d) SLMP-4 films.

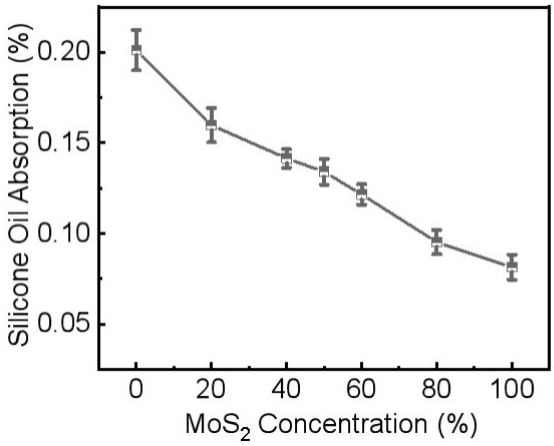

Fig. S12 The silicone oil absorption of SLMP surfaces versus different MoS_2 contents. The silicone oil absorption decreased with increasing MoS_2 content at 20 °C.

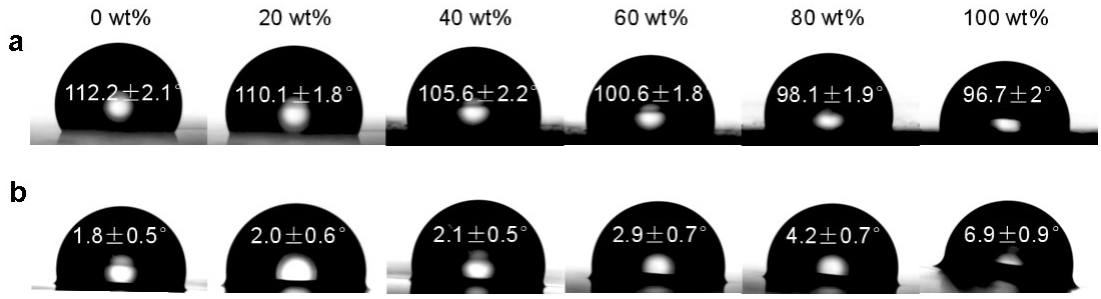

Fig. S13 (a) Water CA photographs and (b) SA photographs on SLMP films containing different MoS_2 contents. CAs decreased, while SA increased with increasing MoS_2 content at 20 °C.

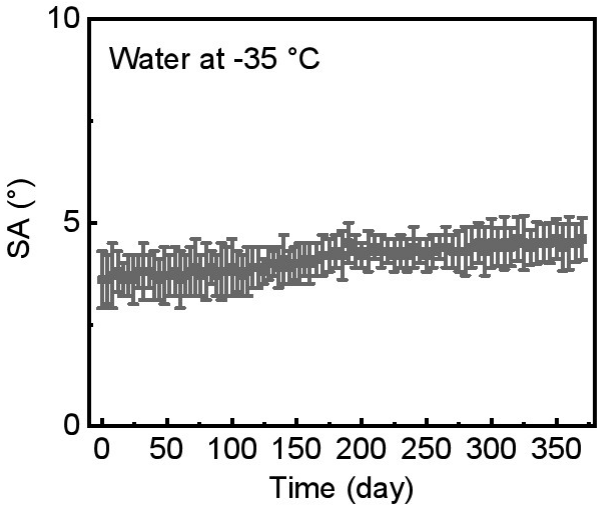

Fig. S14 The SLMP film has a stable SA under low temperature, the SA of water droplets is stable at 3.6° for 370 days at -35 °C.

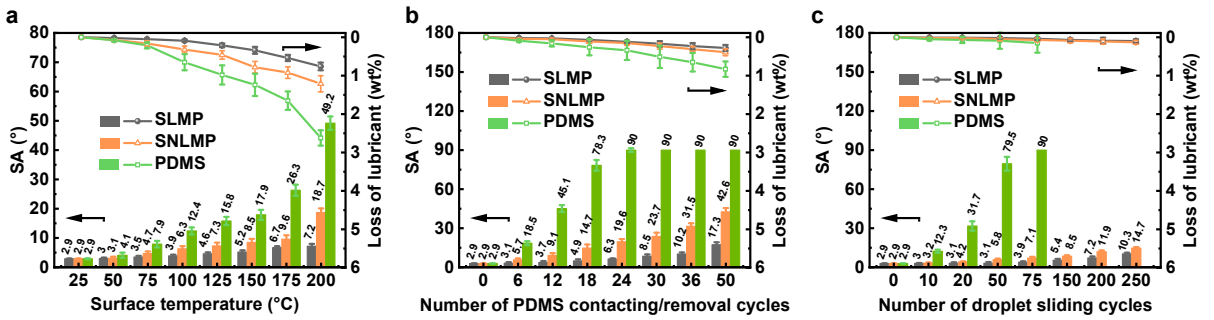

Fig. S15 The slippery stability of SLMP, SNLMP, and slippery PDMS films. (a) The SA and lubricant loss of SLMP, SNLMP, and slippery PDMS films at different surface temperatures. With the increase of surface temperature from 25 to 200 °C, the SLMP film lost only 0.76 wt% silicone oil and its SA increased from 2.9° to 7.2°. The SNLMP film lost 1.21 wt% silicone oil and its SA increased from 2.9° to 18.7°, while the slippery PDMS film lost 2.62 wt% silicone oil and its SA increased from 2.9° to 49.2° at 200 °C. (b) The SA and lubricant loss after repeated pressing/removal of solid PDMS block on samples at a pressure of 25 kPa. The SA of the slippery PDMS film reached 90° at the 24th test, and the loss of lubricant was 0.34 wt% at this time. As the number of contacting/removal cycles increased to 50, the slippery PDMS film lost 0.83 wt% silicone oil. The SLMP film had a slight lubricant loss of 0.28 wt% and showed a low SA of 17.3° at the 50th cycle, and the SNLMP film lost 0.39 wt% silicone oil and its SA increased to 42.6 at the 50th cycle. (c) The SA and lubricant loss after the repeated release of droplets in the same spot. The SLMP and SNLMP films maintained excellent sliding properties and low lubricant loss after testing 250 times in the same spot. For the slippery PDMS film, the SA increased to 90° at the 75th test, and the lubricant loss reached a maximum. The volume of water droplets used above is 2 μL.

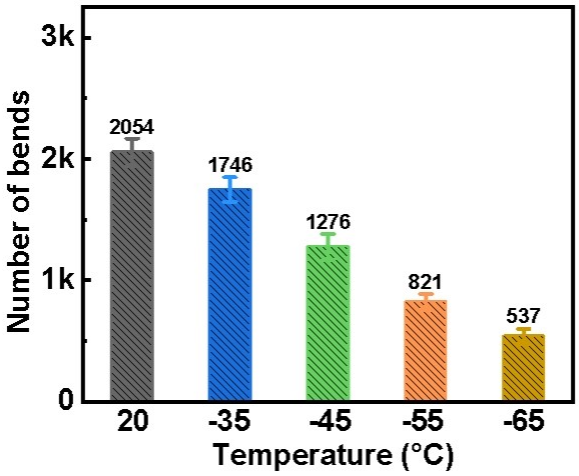

Fig. S16 The bending performance of LMP surface decreases with decreasing temperature from 20 °C to -65 °C.

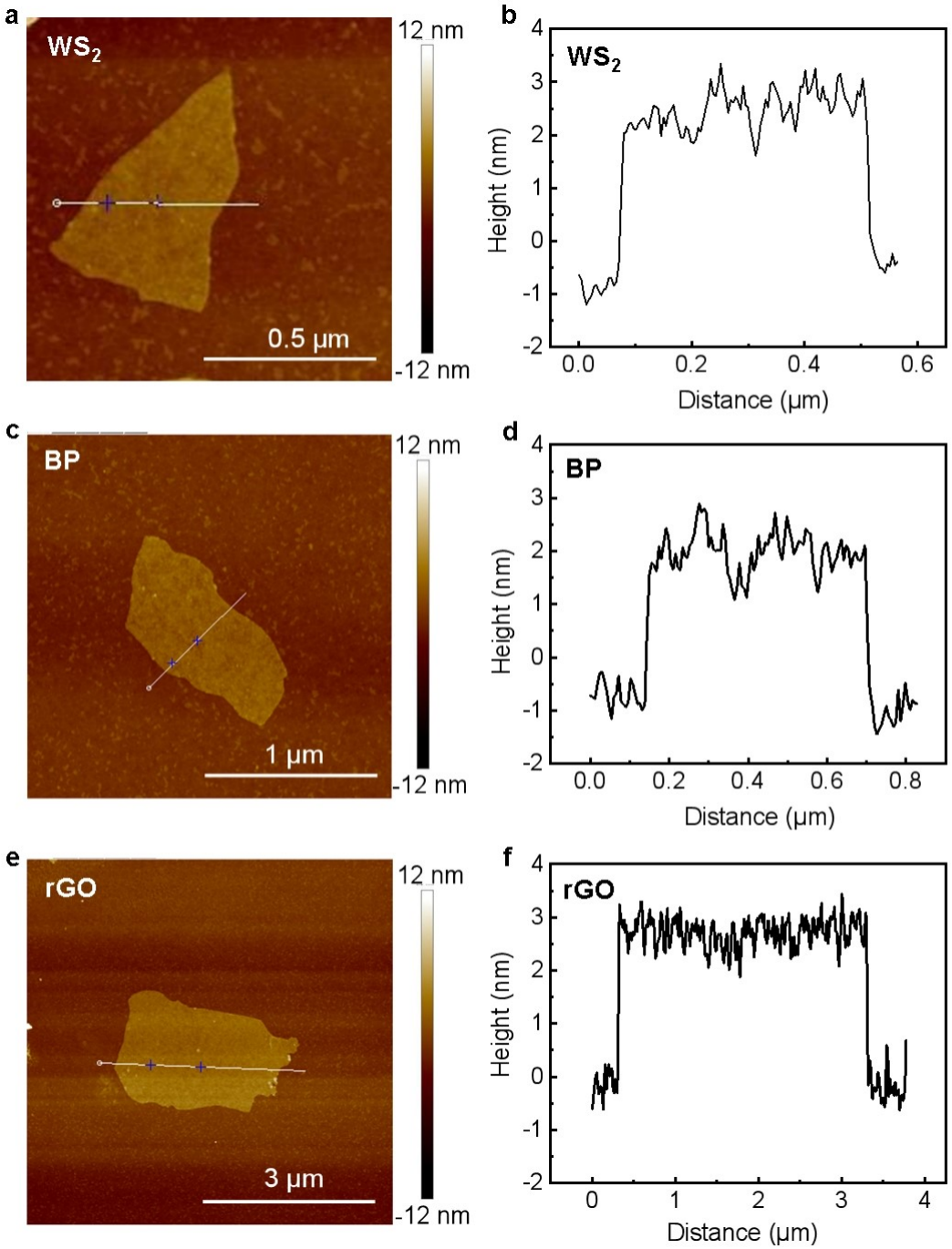

Fig. S17 The AFM image of different nanosheets.

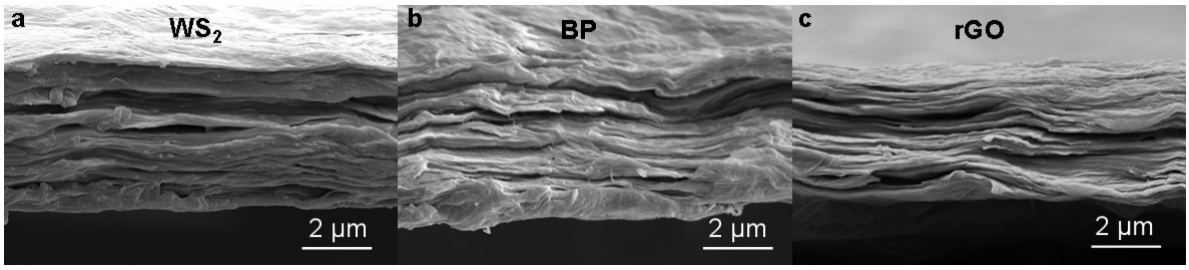

Fig. S18 The morphology of layered films with different nanosheets.

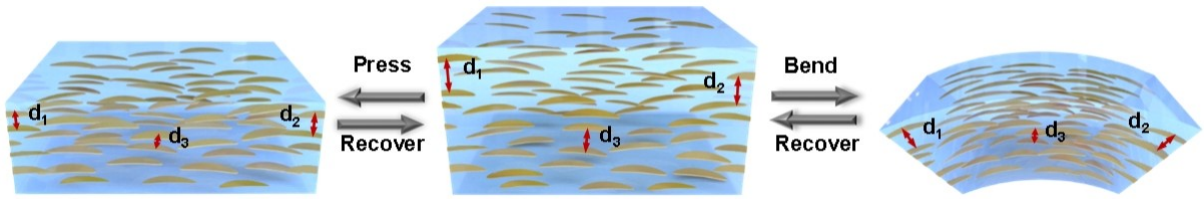

Fig. S19 Schematic of pressure and bending sensing mechanism of the SLMP sensor.

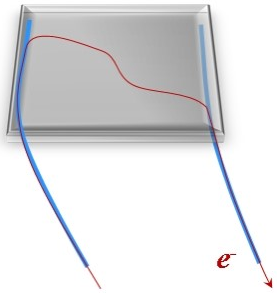

Fig. S20 Schematic illustrations of the SLMP sensor. Conductive wires were anchored by the top and bottom of SLMP film as the source-drain electrodes. On applying external pressure or bend, the compressive deformations of SLMP sensor can induce closer contact of the conductive MoS_2 nanosheets, enabling a larger current.

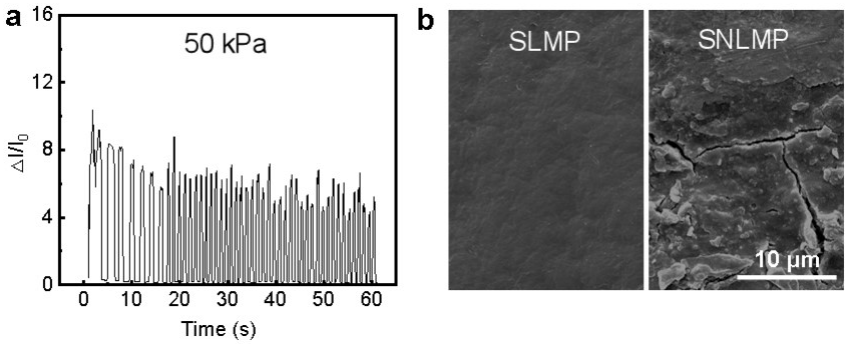

Fig. S21 (a) The pressure sensing signal attenuation of SNLMP sensor under 50 kPa pressure. (b) After 20 times of 50 kPa pressure, the SLMP surface was intact while the SNLMP surface was cracked.

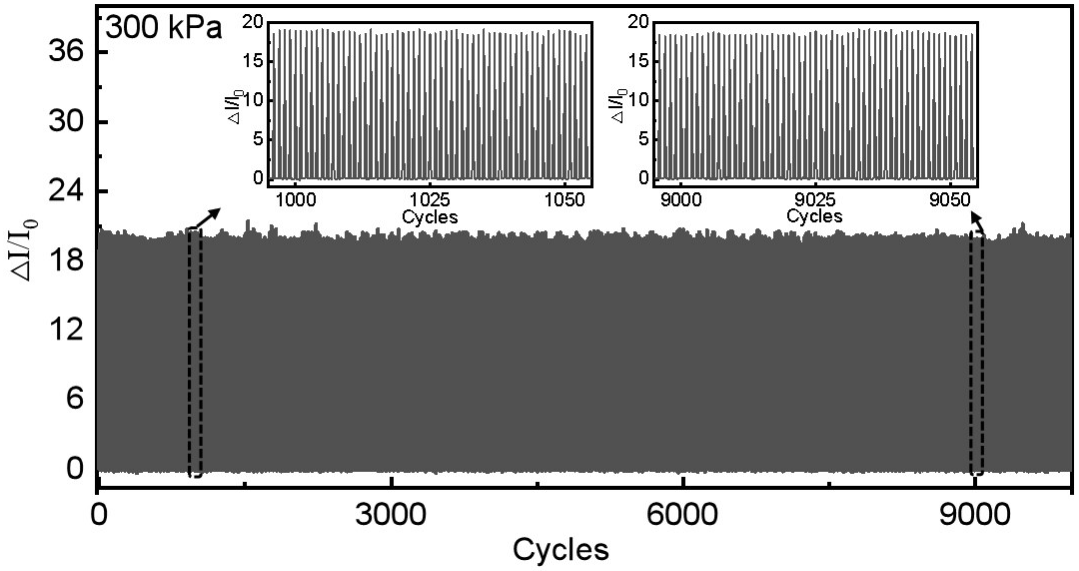

Fig. S22 Relative current changes of SLMP sensor under repeated pressure and release from 0 kPa to 300 kPa for over 10000 cycles, showing excellent durability. The insets show two of 50 cycles after 1000 and 9000 cycles.

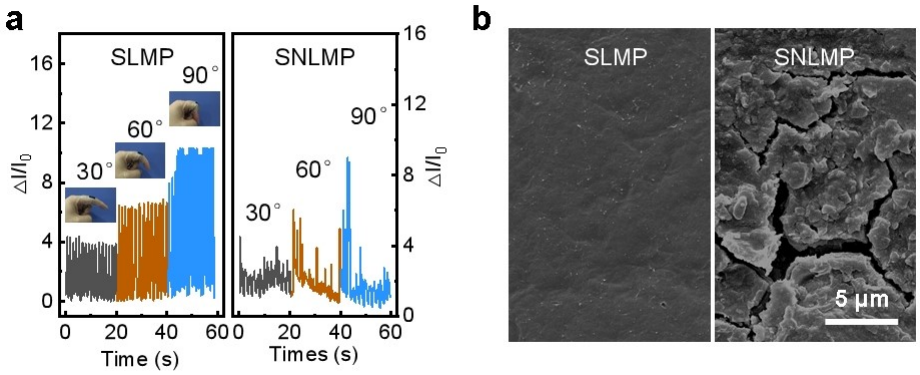

Fig. S23 (a) The bending response of the SLMP sensor (left) and SNLMP sensor (right) attached on a finger knuckle and the corresponding signals with varying degrees of bending. (b) After 20 times of 90° bending, the SLMP surface was intact while the SNLMP surface was cracked.

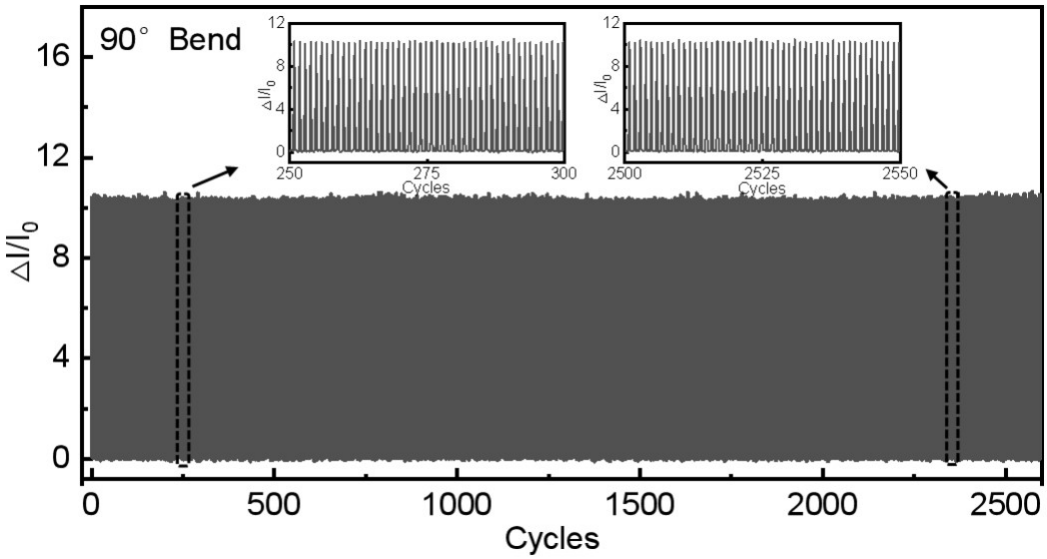

Fig. S24 Bending durability of SLMP sensor. Relative current changes of SLMP sensor under repeated 90° bend and release for over 2600 cycles. The insets show two of 50 cycles after 250th and 2500th cycles.

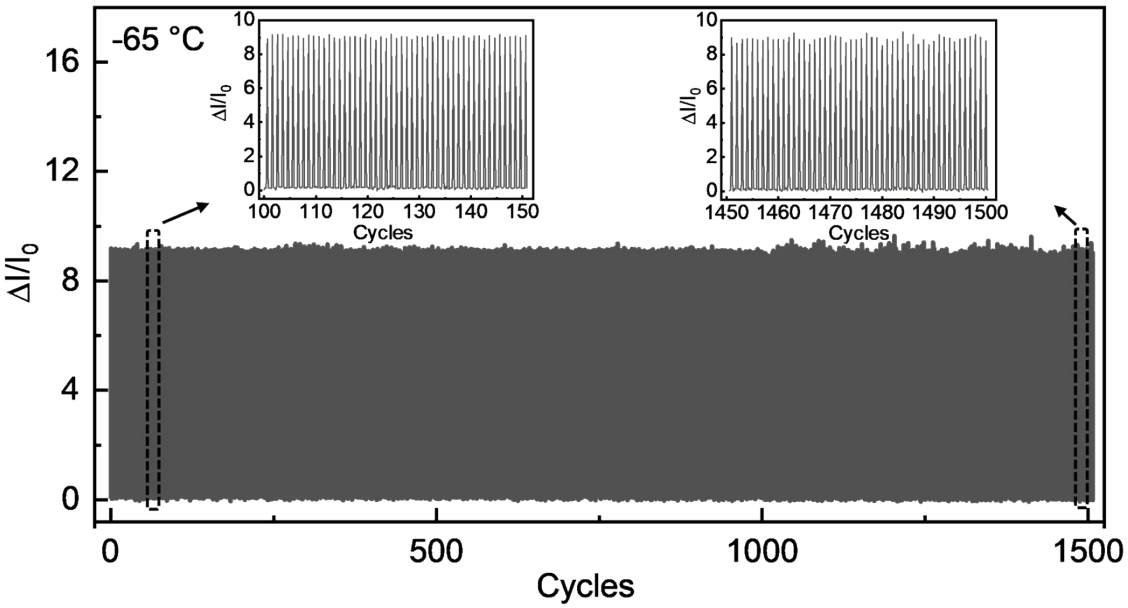

Fig. S25 Low temperature durability of SLMP-4 sensor. Relative current changes of SLMP-4 sensor at -65 °C under repeated 90° bend and release for over 1500 cycles. The insets show two of 50 cycles after 100th and 1450th cycles.

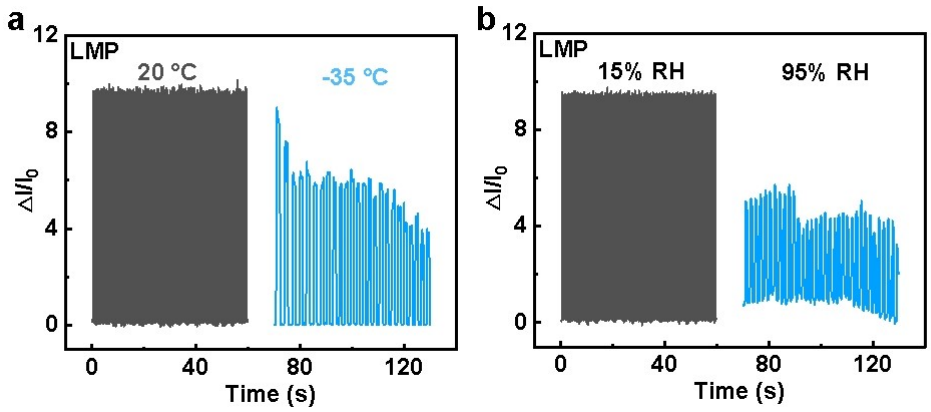

Fig. S26 The lubricant-free LMP sensor shows signal attenuation and unstable disturbances at (a) -35 °C or (b) 95% RH%.

Table S1. Mechanical properties and wettability of layered slippery surfaces prepared from different nanosheets with 60 wt% content at 20 and -35 °C.

Different lamellas	20 ℃					-35 ℃				
	Tensile strength (MPa)	Compressive stress (MPa)	Number of bends	CA (º)	SA (º)	Tensile strength (MPa)	Compressive stress (MPa)	Number of bends	CA (º)	SA (º)
WS_2	85.3±5.9	142.7±10.3	2485±125	95.6±1.2	3.5±1.1	107.2±8.6	188.2±19.5	1986±106	91.1±2.3	5.2±1.3
BP	115.8±8.9	242.5±11.7	2105±142	97.1±2.8	4.1±0.8	143.3±10.5	351.7±15.1	1592±121	92.5±1.7	7.7±1.6
rGO	198.7±7.2	397.1±23.9	2741±105	101.4±2.4	3.0±1.2	235.9±14.7	529.2±24.9	2492±116	96.2±3.6	4.9±1.1

Table S2. Mechanical properties of non-layered slippery surfaces prepared from different nanosheets at 20 and -35 °C.

Different lamellas	20 °C			-35 °C		
	Tensile strength (MPa)	Compressive stress (MPa)	Number of bends	Tensile strength (MPa)	Compressive stress (MPa)	Number of bends
WS_2	38.7±3.5	108.7±5.7	139±23	64.8±5.2	133.6±14.1	88±34
BP	49.1±5.1	197.2±9.1	215±33	81.3±7.4	302.7±21.7	103±21
rGO	108.5±9.7	317.5±14.3	581±58	147.2±12.6	441.5±28.5	319±32

Table S3. The conductivity of LMP films and SLMP films with 60 wt% MoS_2 content under different pressures.

Conductivity (S/m)	0 kPa	0.5 kPa	1 kPa	10 kPa	20 kPa	50 kPa	100 kPa	200 kPa	320 kPa
LMP	1.22×10^{-6}	5.91×10^{-6}	7.98×10^{-6}	1.09×10^{-5}	1.35×10^{-5}	1.52×10^{-5}	1.68×10^{-5}	1.77×10^{-5}	1.81×10^{-5}
SLMP	2.53×10^{-13}	1.31×10^{-12}	1.64×10^{-12}	2.37×10^{-12}	2.67×10^{-12}	2.96×10^{-12}	3.41×10^{-12}	3.67×10^{-12}	3.89×10^{-12}